




Mannose-binding lectin has a direct deleterious effect on ischemic brain microvascular endothelial cells

Laura Neglia, Stefano Fumagalli, Franca Orsini, Adriana Zanetti, Carlo Perego and Maria-Grazia De Simoni 

Abstract

Mannose-binding lectin (MBL), an initiator of the lectin pathway, is detrimental in ischemic stroke. MBL deposition on the ischemic endothelium indicates the beginning of its actions, but downstream mechanisms are not clear yet.

We investigated MBL interactions with the ischemic endothelium by exposing human brain microvascular endothelial cells (hBMECs) to protocols of ischemia. Cells were exposed to hypoxia or oxygen–glucose deprivation (OGD), and re-oxygenated with human serum (HS) or recombinant MBL (rhMBL). Hypoxic hBMECs re-oxygenated with HS showed increased complement system activation (C3c deposition, +59%) and MBL deposition (+93%) than normoxic cells. Super-resolution microscopy showed MBL internalization in hypoxic cells and altered cytoskeletal organization, indicating a potential MBL action on the endothelial structure. To isolate MBL effect, hBMECs were re-oxygenated with rhMBL after hypoxia/OGD. In both conditions, MBL reduced viability (hypoxia: –25%, OGD: –34%) compared to conditions without MBL, showing a direct toxic effect. Ischemic cells also showed greater MBL deposition (hypoxia: +143%, OGD: +126%) than normoxic cells. These results were confirmed with primary hBMECs exposed to OGD (increased MBL-induced cell death: +226%, and MBL deposition: +104%). The present findings demonstrate that MBL can exert a direct deleterious effect on ischemic brain endothelial cells *in vitro*, independently from complement activation.

Keywords

Ischemic stroke, mannose-binding lectin, endothelium, complement system, neuroinflammation

Received 18 March 2019; Revised 24 July 2019; Accepted 10 August 2019

Introduction

Mannose-binding lectin (MBL) is a pattern recognition receptor that belongs to the collectin family of proteins. It can act as initiator of the lectin pathway (LP) of complement system activation. Data obtained in stroke patients and in experimental models using middle cerebral artery occlusion (MCAo) show that MBL is important in ischemic brain injury.^{1–4} Patients with genetic variants causing functional MBL deficiency (20–30% of the general population) have a better outcome and smaller lesions after ischemic stroke.^{3,4} In rodent models of ischemia, MBL genetic deletion or its pharmacological inhibition lead to a smaller lesion and improved neurological deficits.^{1–3} This evidence underlines an important role for MBL in the pathophysiology of ischemic stroke and shows that this is a druggable pathway.

Recent data point to MBL as a key molecule controlling and coordinating multiple pathogenic cascades during ischemic brain injury.⁵ In fact, while activation of the complement cascade may directly affect brain ischemic injury, evidence is accumulating that other pathways may be involved and the exact mechanisms by which MBL worsens brain injury are not known.

In physiological conditions, MBL, synthesized by the liver, circulates in blood. After ischemic injury, MBL affects the brain hemodynamic response.^{6,7}

Istituto di Ricerche Farmacologiche Mario Negri IRCCS, Milano, Italy

Corresponding author:

Maria-Grazia De Simoni, Istituto di Ricerche Farmacologiche Mario Negri IRCCS, via Mario Negri 2, Milan 20156, Italy.
Email: desimoni@marionegri.it

Our group has recently shown that MBL deficiency is associated with better vascular function, faster blood flow and lower extravasation from vessels to brain parenchyma.⁷ In addition, MBL's action also involves a direct interaction with platelets, a few hours after experimental stroke. MBL drives a platelet inflammatory phenotype and induces the associated release of IL-1 α , which in turn drives vascular inflammation and injury.^{7,8} Later on, IL-1 α favours MBL deposition on the brain ischemic endothelium, sustaining the vascular inflammatory phenotype that drives expansion of the ischemic lesion.⁷ In a murine model of stroke, we previously reported that MBL selectively deposits on the ischemic endothelium and can last at least until 48 h post-stroke.² Since MBL is not synthesized by brain cells and brain ischemia does not induce its gene expression,⁹ deposited MBL that found deposited on ischemic vessels comes from the circulation. MBL deposition is prevented when ischemic mice are treated with an MBL inhibitor injected systemically that provides protection from injury.² Thus, MBL deposition on ischemic endothelium seems to be an important event for MBL-driven damage in ischemic brain injury, though the molecular mechanisms involved and the consequences of this event are not known.

To further explore the mechanisms arising from MBL deposition on ischemic vessels, we set-up a few *in vitro* ischemia/reperfusion injury models using human brain microvascular endothelial cells (hBMECs). These *in vitro* models allowed us to better investigate the MBL interaction with the cerebral ischemic endothelium and the consequences of its deposition. hBMECs were exposed to different severity of ischemic injury by hypoxia or oxygen–glucose deprivation (OGD). During re-oxygenation, ischemic cells were treated with human serum (HS) or recombinant MBL (rhMBL), respectively, to explore MBL actions when the complement machinery is available¹⁰ or those induced directly by MBL. We can report, for the first time, that MBL has a direct cytotoxic effect, independent of complement activation, on ischemic brain microvascular endothelial cells, and this is another mechanism through which MBL can drive brain injury following ischemic stroke.

Materials and methods

Cell culture

Immortalized hBMECs (Innoprot). Cells were seeded on black 96-well μ -plates (ibidi, Germany) with optically clear flat bottom, suitable for fluorescence microscopy. Plates were coated overnight before use, with fibronectin (Sigma) 15 μ g/mL in Dulbecco's phosphate buffer saline (DPBS, Euroclone). Cells were cultured in

MCDB 131 (Gibco) supplemented with 5% fetal bovine serum (FBS, Euroclone), 2 mM L-glutamine (Gibco), penicillin/streptomycin (P: 100 U/mL-S: 100 U/mL, Sigma), 1 μ g/mL hydrocortisone (Sigma), 50 μ g/mL endothelial cell growth supplement (ECGS, Sigma), and kept at 37°C, with 5% CO₂ and 90% humidity.

Primary hBMECs (isolated by ScienceCell Research Laboratories and purchased from Innoprot). Cells were cultured as previously described.⁷ Briefly, cells were seeded on fibronectin-coated black 96-well μ -plates (ibidi, Germany) with optically clear flat bottom, suitable for fluorescence microscopy. Cells were cultured with endothelial cell medium supplemented with FBS, ECGS and penicillin/streptomycin solution (all from Innoprot).

In vitro ischemia models

Hypoxia and re-oxygenation. Immortalized hBMECs were transferred into an hypoxic chamber (Ruskin Invivo2 400, UK) at +37°C, and maintained in deoxygenated culture medium (MCDB-131 supplemented as described above) at the following gas concentrations: O₂ 0.5%, CO₂ 5% and N₂ 94.5% for 16 h. Deoxygenated culture medium was obtained by leaving growth medium in a Petri dish inside the hypoxic chamber for 7 h before use. Control cells were maintained in fresh culture medium in a normoxic incubator. After 16 h, hypoxic cells were taken out of the hypoxic chamber, washed twice with DPBS and re-oxygenated for 4 h in a normoxic incubator. During re-oxygenation, normoxic and hypoxic cells were exposed to 30% HS (Innovative Research) or 10 μ g/mL rhMBL (R&D systems) diluted in culture medium (not supplemented with FBS). At the end of re-oxygenation, cell viability was assessed as detailed below, and then cells were fixed with 4% paraformaldehyde (PFA) in DPBS RT for 15 min. Fixed cells were stored in 0.01 M NaN₃ in PBS 0.01 M at +4°C until immunofluorescence analysis.

OGD and re-oxygenation

Immortalized hBMECs. Immortalized hBMECs were transferred into the hypoxic chamber (at +37°C) and maintained in deoxygenated DMEM without glucose (Gibco), supplemented with 2 mM L-glutamine, 100 U/mL penicillin and streptomycin and 50 μ g/mL ECGS. Cells were kept in the hypoxic chamber for 16 h at the following gas concentrations: O₂ 0.5%, CO₂ 5% and N₂ 94.5%. After OGD, cells were re-oxygenated for 4 h in a normoxic incubator. During re-oxygenation, normoxic and OGD cells were exposed to normoglycemic medium (not supplemented with FBS) with 10 μ g/mL rhMBL. At the end, cell viability

was assessed as detailed below, followed by fixation with 4% PFA for 15 min. Fixed cells were stored in 0.01 M NaN_3 in PBS 0.01 M at $+4^\circ\text{C}$ for immunofluorescence analysis.

Primary hBMECs. Primary hBMECs were transferred into the hypoxic chamber (at $+37^\circ\text{C}$) and maintained in deoxygenated DMEM without glucose (Gibco), supplemented with 2 mM L-glutamine and 100 U/mL penicillin and streptomycin. Cells were kept in the hypoxic chamber for 5 h at the following gas concentrations: O_2 0.1%, CO_2 5% and N_2 94.5%. After OGD, cells were re-oxygenated for 48 h (primary hBMECs), in a normoxic incubator. During re-oxygenation, normoxic and OGD cells were exposed to normoglycemic medium (not supplemented with FBS) with 10 $\mu\text{g}/\text{mL}$ rhMBL. At the end, cell death was assessed as detailed below, followed by fixation with 4% PFA for 15 min. Fixed cells were stored in 0.01 M NaN_3 in PBS 0.01 M at $+4^\circ\text{C}$ for immunofluorescence analysis.

Cell viability

Cell viability was assessed with AlamarBlue reagent (Invitrogen). Cells were washed twice with DPBS and incubated with AlamarBlue 1:10 in culture medium (without FBS) for 2 h at 37°C . Fluorescence was measured with a spectrofluorimeter (TECAN plate reader, Infinite M200, Switzerland) using $\lambda_{\text{exc}} = 560 \text{ nm}$ and $\lambda_{\text{em}} = 590 \text{ nm}$.

Cell death

Cell death was assessed by propidium iodide (PI) incorporation.⁷ hBMECs were incubated with PI fluorescent dye (5 $\mu\text{g}/\text{mL}$, Sigma). PI incorporation was measured with a spectrofluorimeter ($\lambda_{\text{exc}} = 535 \text{ nm}$, $\lambda_{\text{em}} = 617 \text{ nm}$; TECAN plate reader, Infinite M200, Switzerland). Cells were then fixed for 30 min at room temperature with 4% PFA. Nuclei were stained with 4'-6-diamidino-2-phenylindole (DAPI, 1 $\mu\text{g}/\text{mL}$, Invitrogen) and fluorescence was measured with a spectrofluorimeter ($\lambda_{\text{exc}} = 355 \text{ nm}$, $\lambda_{\text{em}} = 458 \text{ nm}$). Cell death was expressed as PI over DAPI fluorescence for each well.

Immunofluorescence

Immunofluorescence was done on fixed cells. Nuclei were stained with DAPI (1 $\mu\text{g}/\text{mL}$). For MBL staining, after a blockade with 1% normal goat serum for 1 h, fixed cells were incubated overnight with mouse anti-human MBL (1:100, Hycult Biotechnology). Cells were then incubated with biotinylated anti-mouse (1:200) for 1 h followed by incubation with streptavidin Alexa 647-conjugated (1:100) for 30 min. For F-actin staining,

fixed cells were blocked with 1% bovine serum albumin for 30 min, then incubated with phalloidin Alexa 488-conjugated (1:20, Invitrogen). Apoptotic cells were labelled by terminal deoxynucleotidyl transferase-mediated dUTP nick end labeling (TUNEL) staining using in situ cell death detection kit (Roche, Mannheim, Germany) according to the manufacturer instructions, as previously described.¹¹ For zona occludens-1 (ZO-1) staining, after a blockade with 3% normal goat serum for 30 min, cells were incubated overnight with polyclonal rabbit anti-ZO-1 (1:100, Invitrogen) and then with anti-rabbit Alexa594-conjugated (1:100) for 1 h.

Confocal microscopy and quantitative analysis. Images for MBL on hBMECs were obtained by acquiring a $2.5 \times 2.5 \text{ mm}$ field in the center of each well. Acquisitions were done by microscopy with a confocal scanning A1 unit (Nikon), managed by 'NIS-elements' software. Cells were illuminated with 405 nm (nuclei) and 640 nm (MBL) lasers; 512×512 pixel images were acquired with a $20\times$ objective, over a $10 \mu\text{m}$ stack, with $2.65 \mu\text{m}$ step size, and stitched with 15% overlay. To avoid bleed-through effects, a sequential scanning mode was used. After background subtraction, the fluorescent signal for MBL was quantified by ImageJ software and normalized on nuclei number present in the quantified area. Graphic elaboration of images was done with GIMP software.

Super-resolution microscopy. Structured illumination microscopy (SIM) was done on a Nikon SIM system with a $100 \times 1.49 \text{ NA}$ oil immersion objective or a 60×1.27 numerical aperture water immersion objective (for F-actin quantification), managed by NIS elements software. Cells were imaged at laser excitation of 405 nm for nuclei, 488 nm for F-actin and 640 nm for MBL with a 3D-SIM acquisition protocol. Fourteen-bit images sized 1024×1024 pixels with a single pixel of $0.030 \mu\text{m}$ ($100\times$) or $0.036 \mu\text{m}$ ($60\times$) were acquired in a gray level range of 0–4000 to exploit the linear range of the camera (iXon ultra DU-897U, Andor) at 14-bit and to avoid saturation. Raw and reconstructed images were analyzed with the SIMcheck plugin of ImageJ.¹² For F-actin quantification, 16 cells from four wells per condition were acquired and analyzed. Cells were sampled based on a confocal image at $60\times$ that served as reference to distinguish MBL+ from MBL– cells in the hypoxic wells. SIM images were quantified with ImageJ. Briefly, a region of interest was drawn including the cell cytoplasm but not the nucleus. Background noise was normalized throughout the samples and F-actin filaments were selected by signal segmentation followed by the skeletonize function. Skeletonized filaments longer than 30 nm were selected

and super-imposed by a grid with lines 3 μm apart. Filament touchings with the grid were quantified by an algorithm.¹³ Data were expressed as touchings per filament. Images were finally elaborated with GIMP.

C3c cell-surface ELISA

Fixed cells were washed three times with washing buffer (10 mM Tris-HCl, 140 mM NaCl, 5 mM CaCl_2 , 0.05% Tween 20, pH 7.4) and incubated with BSA (1% in washing buffer) for 2 h at RT. After three washings, cells were incubated with a rabbit polyclonal anti-human C3c (Dako, A0062) diluted 1:5000 in washing buffer, for 1 h 30 min at RT. After washing, cells were incubated with an alkaline-phosphatase-labeled goat anti-rabbit IgG antibody (Sigma A-3812) diluted 1:1000 in washing buffer for 1 h 30 min at RT. Cells were then washed and the assay was developed using substrate solution (Fast p-Nitrophenyl Phosphate tablets, Sigma). The absorption was read at OD 405 nm using the spectrofluorimeter (TECAN plate reader, Infinite M200, Switzerland).

Real-time RT-PCR

Total RNA was extracted from cells at the end of the 4 h re-oxygenation using the miRNeasy kit (Qiagen) according to the manufacturer's instructions. Samples of total RNA (100 ng) were treated with DNase (Applied Biosystems, Foster City, CA, USA) and reverse-transcribed with random hexamer primers using multiscribe reverse transcriptase (TaqMan reverse transcription reagents, Applied Biosystems, Foster City, CA, USA). Primers were designed to span exon junctions in order to amplify only spliced RNA, using PRIMER-3 software (<http://frodo.wi.mit.edu/>) based on GenBank accession numbers (β -actin: NM_001101.5, *MBL2*: NM_000242.2). The same starting concentrations of cDNA template were used in all cases. Real-time PCR was done using Power SYBR Green according to the manufacturer's instructions (Applied Biosystems). β -actin was used as reference gene and relative gene expression levels were determined according to the $\Delta\Delta\text{Ct}$ method (Applied Biosystems). Data are presented as the -fold change compared to the positive control HepG2 cells expressing *MBL2*. Primer sequences: *MBL2* fwd: tgtagctctcaggcatcaa, rev: tgaagcctctgagcccttg; β -actin fwd: ccagctcaccatgatgatg, rev: atgccggagccgtgtgc.

Statistical analysis

Wells containing cells were randomly allocated to treatments. Subsequent immunohistological evaluations

were done by blinded investigators. Data are reported as box plots and 10th and 90th percentiles. Groups were compared by analysis of variance (ANOVA) and post hoc test, as indicated in each figure legend. The parametric or non-parametric test was selected after a Kolmogorov-Smirnov test for normality to assess whether groups met normal distribution. The constancy of variances was checked by Bartlett's test. Data with equal variances were analysed with two-way ANOVA followed by Sidak's multiple comparison, one-way ANOVA followed by Tukey's multiple comparisons or unpaired t-test. Welch's-corrected ANOVA followed by Games-Howell test or Welch's corrected t-test was used for normally distributed data with unequal variances. Group size was defined *pre hoc* using the formula: $n = 2\sigma^2 f(\alpha, \beta) / \Delta^2$ (sd in groups = σ , type I error $\alpha = 0.05$, type II error $\beta = 0.2$, percentage difference between groups $\Delta = 25$). The standard deviation between groups was calculated on the basis of previous experiments, with cell viability as the main output parameter, and resulted in $\sigma = 15.41$, yielding $n = 6.003$.

Availability of data and material

The datasets generated during the current study are available in the Figshare repository, doi: 10.6084/m9.figshare.7851296.

Results

HS induces complement pathway activation and MBL deposition on ischemic hBMECs

Immortalized hBMECs were exposed to hypoxia followed by re-oxygenation with or without 30% HS (Figure 1(a)). This percentage of HS was used to show the role of the LP in a model of oxidative stress in HUVEC.^{14,15} Hypoxic cells re-oxygenated with HS showed lower viability than control cells exposed to HS (-44%) or hypoxic cells not exposed to HS (-33%, Figure 1(b)). Since serum contains the complete complement system machinery,¹⁰ we examined complement system activation by quantifying C3c active fragment deposition on immortalized hBMECs. Active C3c fragments arising from C3 cleavage by convertases or serin-proteases were detected by a cell-surface ELISA. C3c deposition on hBMECs was significantly higher (+59%) after hypoxia than normoxic cells exposed to serum (Figure 1(c)), indicating the activation of the proteolytic pathway. We next investigated if our ischemia reperfusion model could detect deposition of MBL on hypoxic cells. As expected, MBL was not observed on cells re-oxygenated without 30% HS, while its presence was

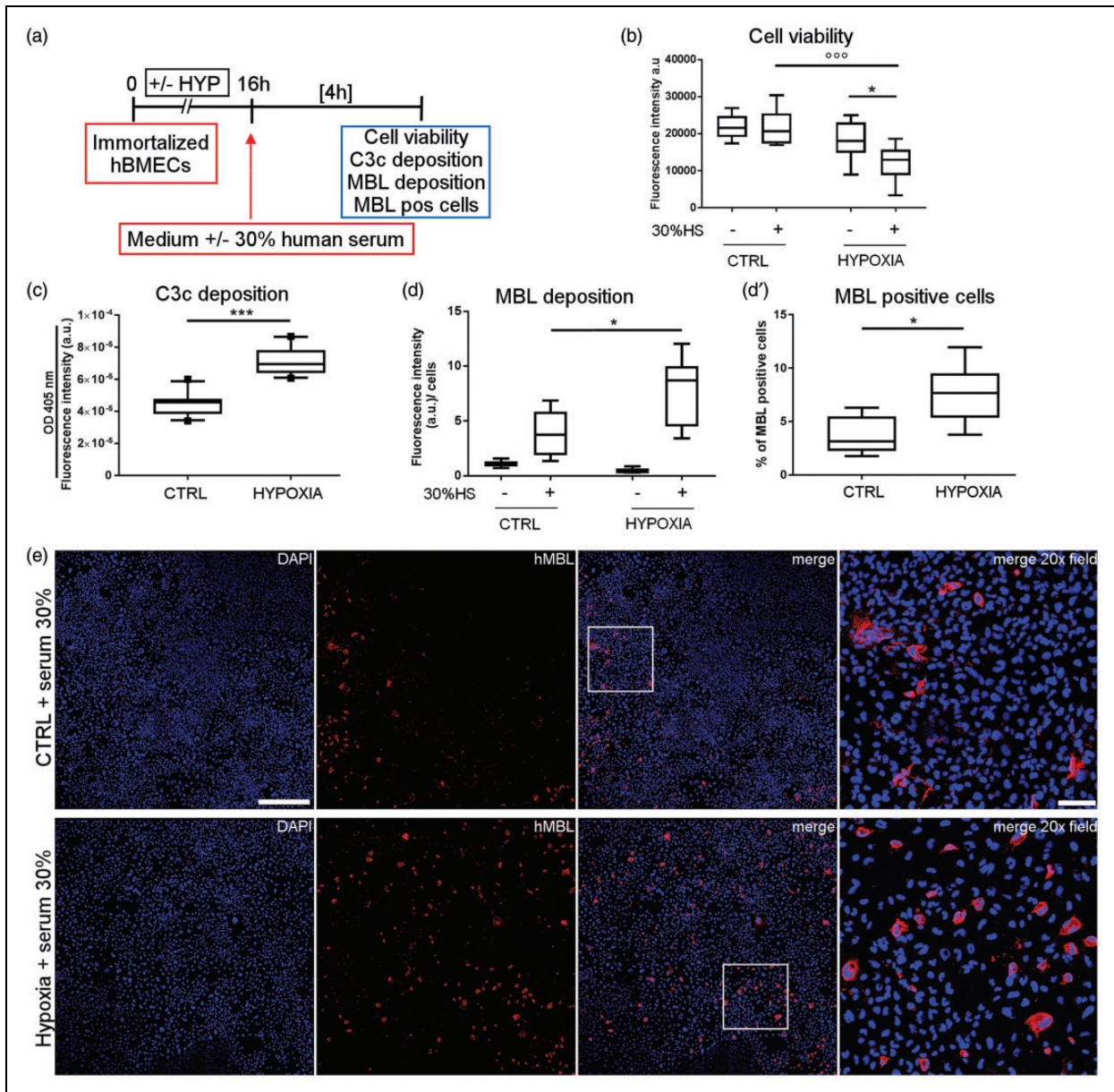


Figure 1. Exposure to human serum induces complement system activation and MBL deposition on hypoxic hBMECs. Immortalized hBMECs exposed to 16 h of hypoxia or not (CTRL) were re-oxygenated with or without human serum diluted 30% in culture medium (30% HS) for 4 h (a). Cell viability was slightly decreased after hypoxia (b). Exposure to 30% HS further reduced cell viability after hypoxia (b). Data are reported as box plots and 10th and 90th percentiles, $n = 7-8$. Two-way ANOVA followed by Sidak's multiple comparison test, $*p < 0.05$, $^{\circ\circ\circ}p < 0.001$. With human serum active C3c fragments, indicating complement activation, increased more on hypoxic than CTRL cells, as measured by cell-surface ELISA, which selectively recognizes C3c fragments (c). Data are reported as box plots and 10th and 90th percentiles, $n = 10$, unpaired t-test, $***p < 0.001$. MBL deposition was greater on hypoxic than CTRL cells exposed to 30% HS, measured as fluorescence intensity normalized on nuclei number (d), as well as the number of MBL-positive cells (d'). Cells not exposed to 30% HS showed no MBL presence (d). Data are as box plots and 10th and 90th percentiles, $n = 6-7$ (CTRL + 30% HS, HYPOXIA + 30% HS), $n = 3$ (CTRL - 30% HS, HYPOXIA - 30% HS), Welch corrected unpaired t-test, $*p < 0.05$ (d, d'). a.u. = arbitrary unit (b, c, d). Confocal images showing MBL (red) after exposure to serum in control (CTRL + serum 30%) and hypoxic (Hypoxia + serum 30%) cells (e, nuclei are blue, scale bar 500 μm ; merge 20 \times field relative to the insert, scale bar 100 μm).

greater on hypoxic cells than on control cells after exposure to 30% HS (+93% vs. CTRL, Figure 1(d) and (e)), indicating MBL deposition. The increased deposition was related to a larger number of MBL-positive cells (7.5% of total cells) compared to the control condition (CTRL, 3.7% of total cells, Figure 1(d') and (e)).

MBL is internalized by ischemic hBMECs showing disorganization of the cytoskeleton

Next, we aimed to clarify whether MBL deposition was localised on cell surfaces and/or inside the cytoplasm. We did confocal and super-resolution SIM analysis on immortalized hBMECs exposed to hypoxia and re-oxygenated with HS (Figure 2(a) to (c)). Confocal images showed MBL clustering around the nucleus in hypoxic cells, suggesting possible intracellular localisation (Figure 2(b)). Super-resolution images obtained by SIM demonstrated that MBL was localised both on the cell surface and inside the cytoplasm, MBL being on the same focal plane as F-actin filaments forming the cytoskeleton (Figure 2(c)). Labeling F-actin filaments with phalloidin showed that normoxic hBMECs re-oxygenated with serum formed a regular layer, while hypoxic hBMECs re-oxygenated with serum showed greater spacing between cells and less dense staining for F-actin (Figure 2(d)).

As reported above, 7.5% of total cells after hypoxia and serum exposure showed MBL accumulation in the cytoplasm. We therefore selected these cells and analyzed whether intracellular MBL presence induced structural changes to the cytoskeleton, as suggested by the fainter F-actin signal in these cells than normoxic or hypoxic MBL-negative cells (Figure 2(d')). F-actin filaments were identified on SIM images and quantified by recording their touchings with superimposed grid (Figure 2(e)). There were fewer touchings per filament in hypoxic MBL-positive cells (0.91 ± 0.34 , mean \pm sd) compared with normoxic (1.29 ± 0.44) or hypoxic MBL-negative (1.36 ± 0.38 , Figure 2(f)) cells. The total number of F-actin filaments (normoxic: 70.74 ± 25.37 ; hypoxic MBL-positive: 68.38 ± 32.86 ; hypoxic MBL-negative: 90.58 ± 24.73) or average filament size (normoxic: $274.30 \text{ nm} \pm 80.46$; hypoxic MBL-positive: $247.40 \text{ nm} \pm 63.65$; hypoxic MBL-negative: $300.10 \text{ nm} \pm 67.38$) did not differ significantly across groups (Figure 2(g) and (g')), indicating that hypoxic cells with MBL internalization had disorganized cytoskeleton rather than filament loss. As expected, hypoxia induced apoptosis (Figure 2(h), TUNEL-positive cells, arrowheads). Every cell showing MBL internalization was apoptotic (Figure 2(h), arrows), suggesting that viability was particularly affected in these cells.

MBL plays a direct toxic effect on ischemic hBMECs

To isolate the effect of MBL during re-oxygenation, ischemic endothelial cells were exposed to rhMBL in a culture medium which did not contain HS or complement factors. Immortalized hBMECs were exposed to hypoxia followed by re-oxygenation with or without rhMBL ($10 \mu\text{g/mL}$, Figure 3(a)). Hypoxic cells re-oxygenated with rhMBL showed lower viability than control cells exposed to rhMBL (-47%) or hypoxic cells not exposed to rhMBL (-25% , Figure 3(b)). Hypoxic hBMECs had more MBL deposition ($+153\%$) than control cells after rhMBL exposure (Figure 3(c) and (d)), similarly to what was seen with the native form of the protein in the serum (see Figure 1). Due to the previous observation that re-oxygenation in absence of native MBL did not induce MBL presence (Figure 1(d)), we measured MBL only in cells re-oxygenated with rhMBL. To exclude that MBL deposition occurring on these cells could be due to a de novo expression of the *MBL2* gene, we extracted RNA and performed real-time PCR in control and hypoxic immortalized hBMECs, exposed or not to rhMBL. No *MBL2* expression was detectable in these cells when compared with the positive control HepG2 cells (Figure 3(e), and Supplementary Table 1).

We next used OGD, a more severe model of in vitro ischemia, on hBMECs. OGD-exposed immortalized hBMECs were re-oxygenated with or without rhMBL ($10 \mu\text{g/mL}$, Figure 4(a)). OGD reduced the viability of immortalized hBMECs (-53% vs. CTRL), even more so by re-oxygenation with rhMBL (-72% vs. CTRL + rhMBL, -34% vs. OGD - rhMBL, Figure 4(b)). In addition, OGD hBMECs had more MBL deposition ($+126\%$) than control cells after exposure to rhMBL (Figure 4(c) and (d)).

To mimic physiological conditions better, we then did OGD followed by re-oxygenation and exposure to rhMBL on primary hBMECs (Figure 5(a)). OGD significantly increased the death of primary hBMECs ($+558\%$ vs. CTRL), and this was worsened by the addition of rhMBL ($+643\%$ vs. CTRL + rhMBL, $+226\%$ vs. OGD - rhMBL, Figure 5(b)). OGD primary hBMECs had a significantly greater deposition of MBL ($+104\%$) than normoxic cells exposed to rhMBL (Figure 5(c) and (d)). High magnification images of double-immunofluorescent staining for rhMBL and ZO-1 showed that MBL staining was scattered in CTRL cells, but clustered inside the cell bodies after OGD (Figure 5(e)).

Discussion

Previously works have demonstrated that MBL is involved in brain ischemic injury in humans^{3,4} and in

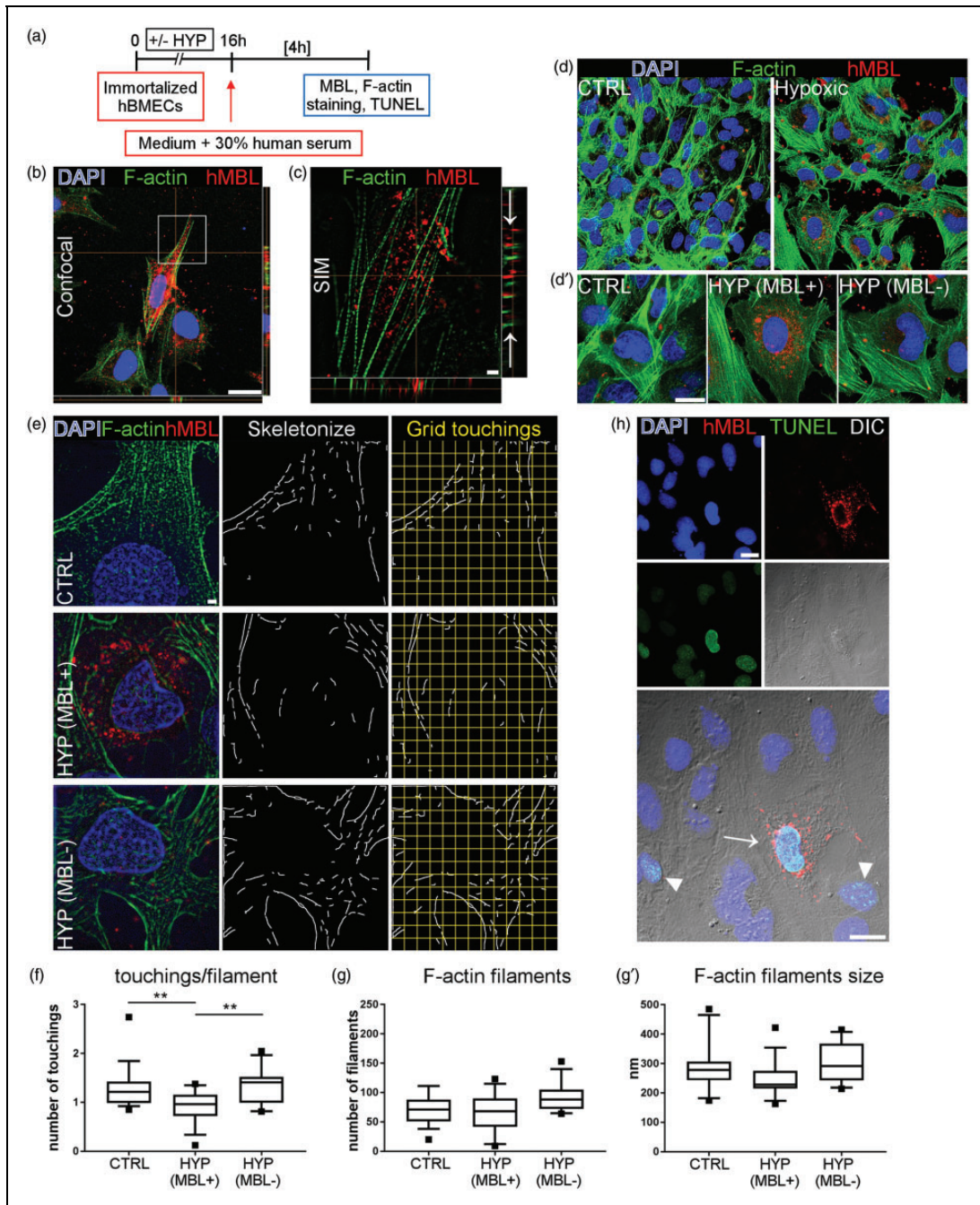


Figure 2. MBL is localized inside hypoxic hBMECs and is associated with cytoskeletal disorganization. Normoxic or hypoxic immortalized hBMECs undergone re-oxygenation in the presence of human serum were analyzed for MBL sub-cellular distribution and cytoskeletal organization (a). Confocal image shows MBL (red) clustering in hypoxic cells labeled with phalloidin (F-actin, green) to stain the cytoskeleton (b, nuclei are blue, scale bar 20 μ m). Super-resolution SIM imaging relative to the insert in B shows that MBL is internalized in the cytoplasm, being on the same focal plane as F-actin filaments, visible in the z projection (arrows in c, scale bar 2 μ m). With confocal microscopy, F-actin staining showed that normoxic (CTRL) hBMECs formed a regular layer, while hypoxic hBMECs had greater spacing between cells and less dense staining for F-actin (d). Hypoxic cells presenting MBL cytoplasmic accumulation (HYP MBL+) showed fainter F-actin staining than normoxic (CTRL) or hypoxic cells without MBL (HYP MBL-) (d', scale bar 20 μ m). SIM images of F-actin were used to assess the cytoskeletal structure in CTRL, HYP MBL+ and HYP MBL- cells after F-actin skeletonization and 3 μ m-spaced grid superimposition (e, scale bar 2 μ m). There were fewer grid touchings per F-actin filament in HYP MBL+ cells than CTRL or HYP MBL- (f). Data are reported as box plots and 10th and 90th percentiles, $n = 16$ cells from four wells per condition. One-way ANOVA followed by Tukey's multiple comparison test, $**p = 0.01$. The number of F-actin filaments per cell (g) or filament average size (g') did not differ significantly across groups. Some hypoxic cells re-oxygenated with serum (H, arrowheads) and all those showing MBL internalization (H, arrows) were apoptotic (TUNEL positive cells are green, MBL is red, nuclei are blue, phase-contrast image DIC, scale bars 20 μ m).

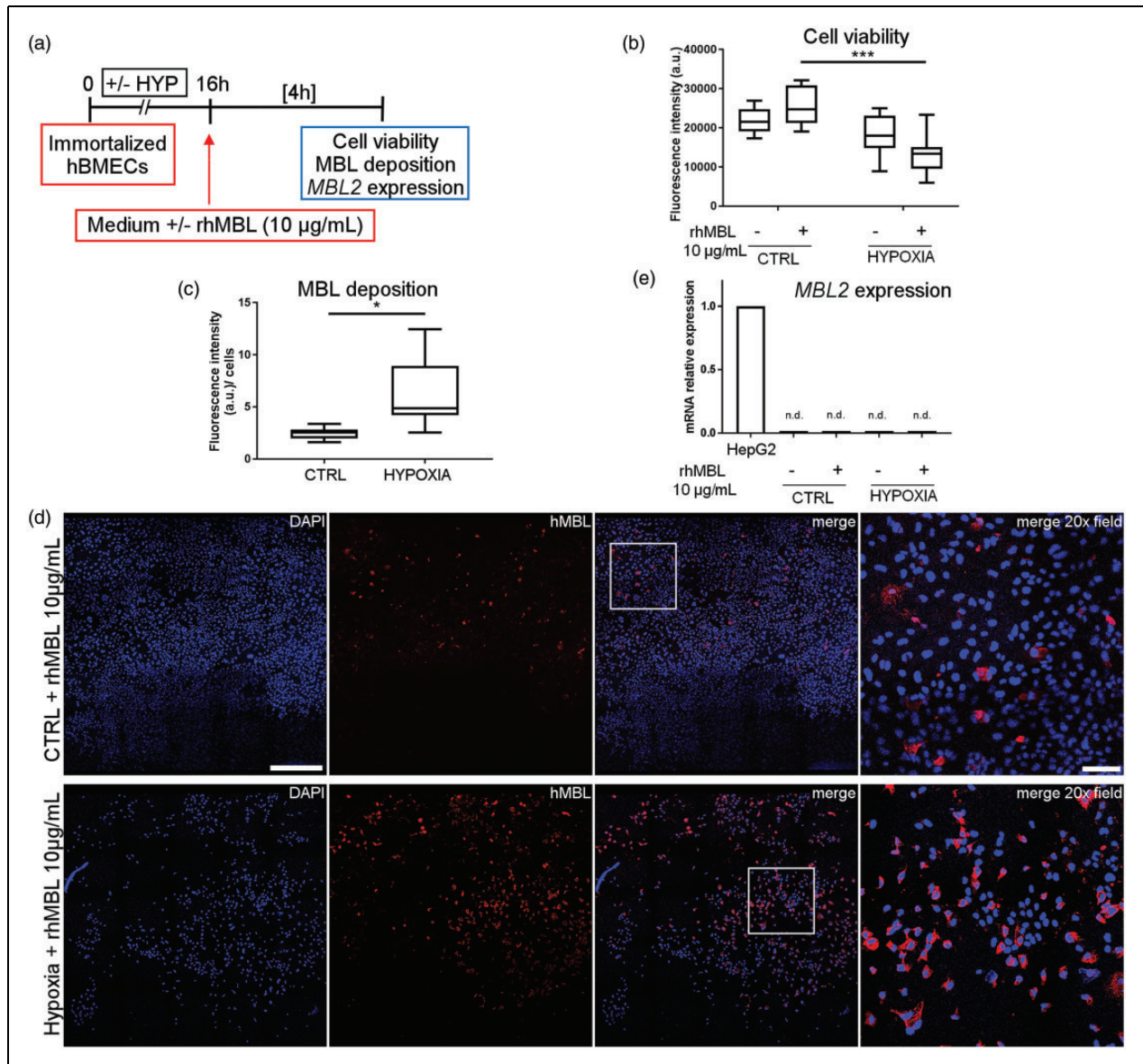


Figure 3. rhMBL reduces cell viability and deposits on immortalized hBMECs following hypoxia. Immortalized hBMECs exposed to 16 h of hypoxia or not (CTRL) were re-oxygenated with or without rhMBL (10 µg/mL) for 4 h (a). Cell viability was slightly decreased after hypoxia (b). The application of rhMBL further reduced cell viability after hypoxia (b). Data are reported as box plots and 10th and 90th percentiles, $n = 7-8$. Two-way ANOVA followed by Sidak's multiple comparison test, $***p < 0.001$. Hypoxic cells re-oxygenated with rhMBL (HYPOXIA) had greater MBL deposition than control cells exposed to rhMBL (CTRL) as measured as fluorescence intensity normalized on nuclei number (c). Data are reported as box plots and 10th and 90th percentiles, $n = 7$, Welch corrected t-test, $*p < 0.05$. a.u. = arbitrary unit (b, c). Confocal images showing MBL (red) presence in control (CTRL + rhMBL 10 µg/mL) and hypoxic (Hypoxia + rhMBL 10 µg/mL) cells (d, nuclei are blue, scale bar 500 µm; merge 20× field relative to the insert, scale bar 100 µm). *MBL2* gene expression was not detectable in immortalized hBMEC (n.d.: CTRL ± 10 µg/mL rhMBL; HYPOXIC ± 10 µg/mL rhMBL) when compared to HepG2 cells used as positive control (e, data reported as bars and presented as -fold change compared to the positive control HepG2 cells).

experimental models.¹⁻³ After experimental stroke, MBL deposits on the ischemic endothelium. In experimental models, this occurs starting 6 h after injury, up to at least 48 h.² Strategies to prevent or counteract this are protective, showing its pathophysiological importance. MBL acts as a circulating pattern recognition

receptor which recognizes sugar moieties expressed on the surface of injured cells by its carbohydrate recognition domain (CRD). Upon binding, the associated serin proteases (MASPs) trigger the activation of the complement cascade. At present, the molecules recognized by MBL on the ischemic endothelium are not known.

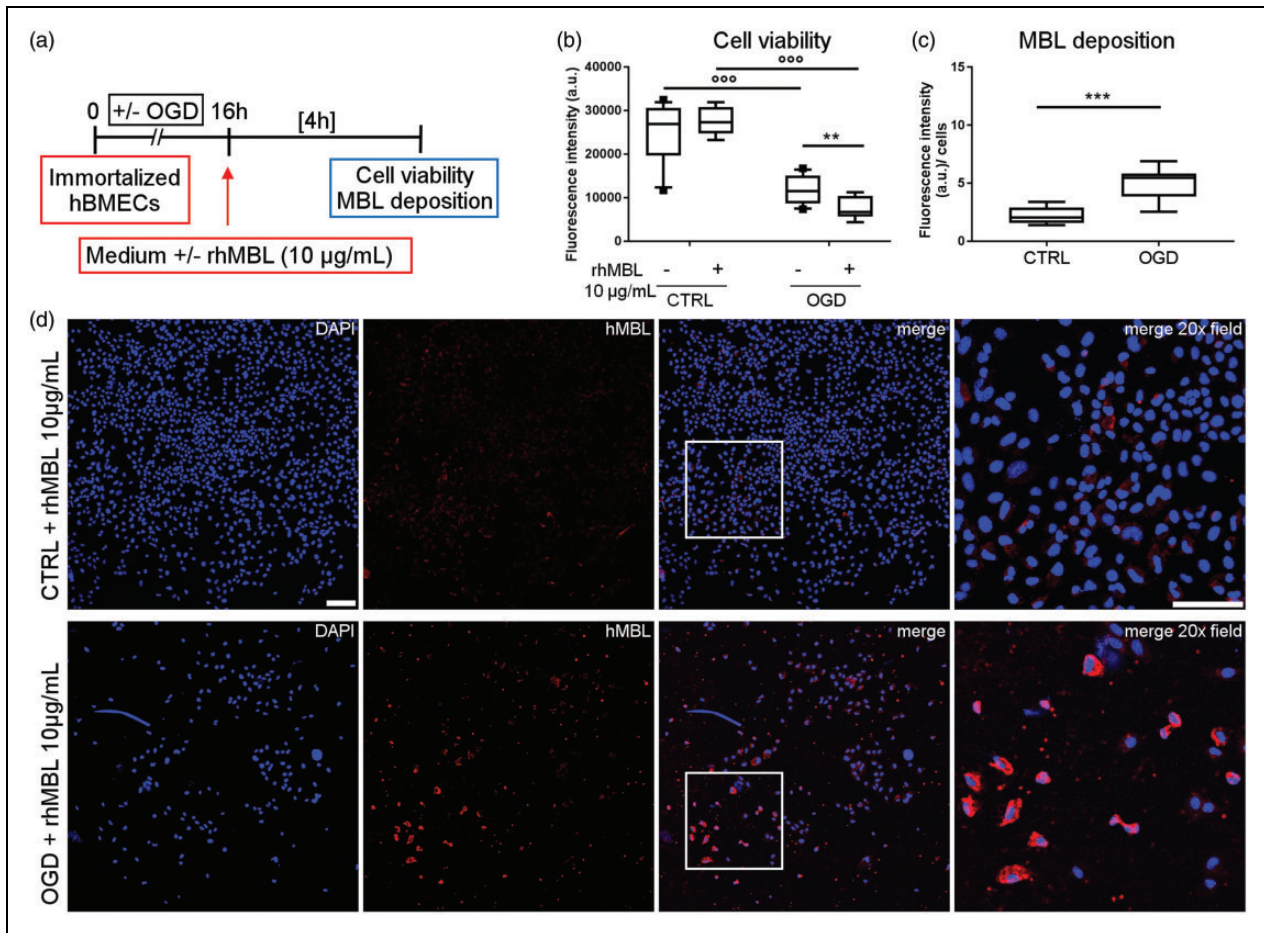


Figure 4. rhMBL reduces cell viability and deposits on immortalized hBMEC after oxygen and glucose deprivation (OGD). Immortalized hBMECs exposed to 16 h of OGD (OGD) or not (CTRL) were re-oxygenated with or without rhMBL (10 µg/mL) for 4 h (a). Cell viability was reduced after OGD (b). Exposure to rhMBL further reduced cell viability after hypoxia (b). Data are reported as box plots and 10th and 90th percentiles, $n = 8-13$, Welch-corrected ANOVA, $^{\circ\circ\circ}p < 0.001$; $^{**}p < 0.01$. MBL deposition was greater on OGD than CTRL cells exposed to rhMBL (c). Data are reported as box plots and 10th and 90th percentiles, $n = 7-8$, unpaired t-test, $^{***}p < 0.001$. a.u. = arbitrary unit (b, c). Confocal images showing MBL (red) in control (CTRL + rhMBL 10 µg/mL) and OGD (OGD + rhMBL 10 µg/mL) cells (d, nuclei are blue, scale bar 125 µm; merge 20× field relative to the insert, scale bar 100 µm).

In addition, although MBL is known to act as initiator of the complement cascade, recent data suggest that it may act as a hub for multiple proinflammatory mechanisms, involving complement and coagulation systems.⁵

To explore the consequences of MBL deposition on ischemic vessels previously reported in ischemic mice,² here we developed in vitro protocols mimicking ischemic injury on brain microvascular endothelial cells. Our study shows that: (1) in the presence of serum, a hypoxic stimulus induces the deposition of endogenous MBL on the endothelium and triggers complement activation; (2) MBL is taken up by endothelial cells where it is associated to cytoskeletal disorganization; (3) MBL has a direct toxic effect on immortalized or primary endothelial cells exposed to hypoxia or to OGD and

this occurs in the absence of serum components, hence independently of complement activation.

As a circulating pattern recognition receptor, MBL is able to recognize molecules or alterations on the surfaces of activated or injured cells. In line with this, we found that MBL deposited on ischemic endothelium more than on control cells. This is in line with what is observed in vivo, where MBL deposits selectively on the vessels pertinent to the ischemic territory in stroke mice. This is further corroborated by studies in patients after traumatic brain injury, showing the vascular presence of MBL in ischemic peri-contusional brain areas, unlike in control specimens from people who died from extra-cranial causes.^{16,17}

In this study, we used hBMECs because brain endothelial cells possess features different from endothelial

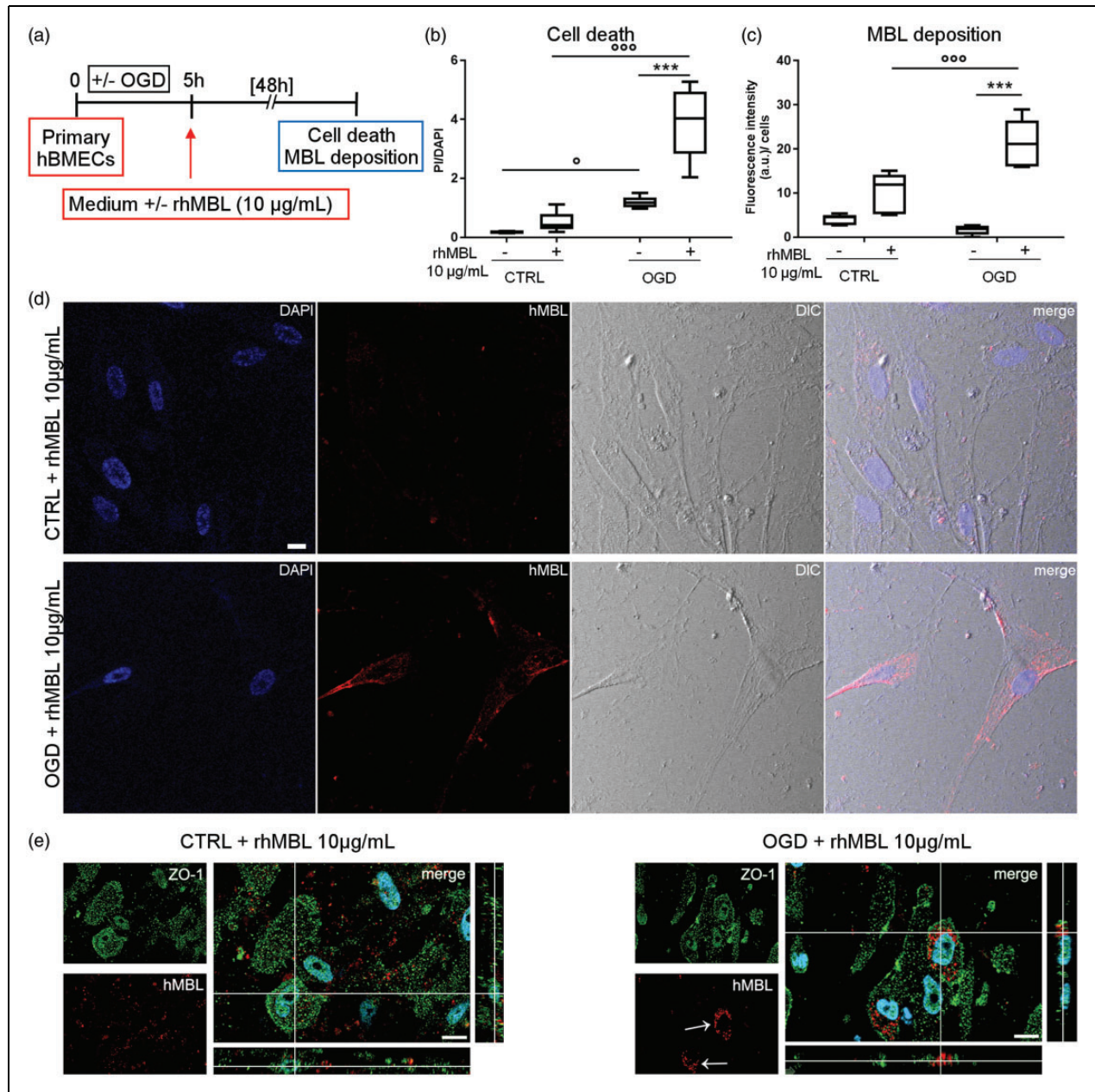


Figure 5. rhMBL reduces cell viability and deposits on primary hBMEC after oxygen and glucose deprivation (OGD). Primary hBMECs subjected to 5 h OGD (OGD) or not (CTRL) were incubated with or without rhMBL (10 µg/mL) for 48 h (a). Cell death increased after 5 h OGD and the application of rhMBL further increased it in primary OGD hBMEC (b). Data are reported as box plots and 10th and 90th percentiles, $n = 6$; Welch-corrected ANOVA, $^{\circ}p < 0.05$, $^{\circ\circ\circ}p < 0.001$; $^{***}p < 0.001$. Increased cell death was associated with greater MBL deposition on OGD than CTRL primary hBMECs exposed to rhMBL (c). Data are reported as box plots and 10th and 90th percentiles, $n = 5-6$; Welch-corrected ANOVA, $^{\circ\circ\circ}p < 0.001$; $^{***}p < 0.001$; a.u. = arbitrary unit. Confocal images show scattered MBL deposition in control cells (CTRL + rhMBL 10 µg/mL) and MBL (red) clustering in OGD cells (OGD + rhMBL 10 µg/mL) after exposure to rhMBL (d, nuclei are blue, phase-contrast image, DIC, scale bar 20 µm). Confocal images for rhMBL and ZO-1 showed a non-specific scattered deposition of rhMBL in CTRL, while an rhMBL clustering in OGD primary hBMECs (green ZO-1, red rhMBL, nuclei are blue, bar 15 µm, e).

cells of other organs and tissues. One important specificity of endothelial cells in the brain is their denser glycocalyx coating compared to other districts.¹⁸ This may affect the ability of complement components, including

MBL, to bind glycoproteins exposed on endothelial cell surfaces. Thus, changes induced by the ischemic stimulus may affect the structural organization of the glycocalyx, and facilitate MBL binding to the endothelium. It is still

not known whether this occurs in other districts. Van der Pol et al.¹⁹ reported MBL deposition and a direct toxic effect on cultured renal tubular epithelial cells in normoxic conditions, which was independent of complement activation and was associated with MBL cellular internalization.¹⁹ However, in their hands MBL did not have any toxic effect on endothelial cells.

We used a high concentration of rhMBL (10 µg/mL) to test its effect on endothelial cells. MBL in healthy subjects shows median values of 2000 ng/mL.²⁰ It operates by binding avidly to precisely spaced repetitive sugar arrays exposed on altered self-cell surfaces. The avidity implies that individual binding events increase the probability of other binding events. Thus, we can hypothesize that high MBL concentrations are needed at the site of action for its functional activation. This is actually what is reported on ischemic vessels after in vivo ischemia, where a strong MBL signal is detectable.^{1,2} Since in our models we could not increase the concentration of rhMBL during time, as it occurs in vivo, we decided to use a higher concentration of rhMBL than the physiological one. This concentration was decided on the basis of previously published in vitro studies showing that the addition of 10 µg/mL MBL to cultured cells promoted a pro-inflammatory phenotype in platelets⁵ and MBL deposition on renal tubular epithelial cells.¹⁹

Importantly, we observed MBL deposition and toxic effects on the ischemic hBMECs using immortalized and primary cell cultures, subjected to different ischemic stimuli (hypoxia or OGD). Immortalized cells are easier to handle and prepare than primary ones, quickly (two to three days) reaching the confluence needed to run the experiments. As such, this model stands as a first-line benchmark for screening molecules targeting MBL. On the other hand, primary cells are more closely related to the physiology of endothelial cells, better mirroring the in vivo properties of the barrier,²¹ and therefore should be used to run the final validation experiment. Having reproduced MBL deposition after in vitro ischemia with both cell types, we found our model suitable for thorough drug screening before moving on to animal models, in line with ethical use of in vivo research.

MBL on the endothelium finally results in its cellular internalization. MBL presence in hBMECs is totally a consequence of MBL contained in the medium during re-oxygenation and subsequently deposited on the cell surface, being *MBL2* gene not expressed in these cells. The consequences of this intracellular localization have been described in phagocytic cells.²² MBL facilitates particle uptake through direct opsonization, not necessarily needing other complement components and/or activation. On inducing phagocytosis, MBL trafficks with its target particle to the phagosome, therefore being internalized.²² In the phagosome, MBL activates the toll-like receptor cascade responsible for myeloid

cell differentiation.²² In our experimental setting, we described MBL uptake by endothelial cells, which have no phagocytic functions, thus suggesting an unexplored MBL action. Super-resolved images obtained by SIM and the quantification of F-actin distribution indicated that after 4-h exposure to serum, MBL is present in cells, showing cytoskeletal disruption. While we do not know the exact mechanisms triggered by internalized MBL, we can speculate that it may recognize molecules such as cytokeratins, which are among its targets,^{15,23} and interfere with their correct assembly, eventually inducing cell death as shown by the apoptotic feature of cells internalizing MBL. We acknowledge that our observations do not completely clarify if MBL entrance in the hypoxic cells is a cause or a consequence of cell damage. In the latter scenario, it is possible that cells damaged by the ischemic injury become permissive to MBL entrance, which in turn enhances cell injury. We cannot rule out other independent effects contributing to cell damage. However, our results with rhMBL strongly suggest its direct detrimental action leading to increased endothelial damage. Indeed in the data obtained in hypoxic or OGD cells – either immortalized or primary – the tested conditions during re-oxygenation differed only for the presence of rhMBL, thus lending support to the hypothesis that MBL presence is sufficient to cause additional damage after ischemia.

In our experimental setting, only a small percentage (7.5%) of cells showed MBL internalization. This event is probably a consequence of the apoptotic feature of these cells, and suggests that we are probably detecting only a part of them, being the others probably already dead.

Stroke is still a large unmet medical need and the identification of new molecular targets is highly desirable for the development of new drugs. What we know about the role of MBL in brain ischemia comes from rodent models where MBL deposits on ischemic vessels and where its inhibition is protective.^{2,7} Patients with genetically defined MBL deficiency have a smaller lesion and a better outcome after stroke.^{3,4} Here the use of human components (serum, MBL and cells) helped get information likely to be clinically transferable. Different lines of evidence indicate the counteraction of MBL deposition on the ischemic vessels as a novel pharmacological approach for ischemic stroke. MBL targeting is expected to provide a wide therapeutic window of efficacy, as its deposition is persistent on the ischemic endothelium, with multiple downstream consequences over time. This kind of pharmacological tool, acting on the endothelial compartment, does not need to access the brain, increasing the likelihood of successful targeting in vivo.

We previously reported that inhibition of the main serine-protease associated with LP activation, MASP-2,

reduced inflammation in a mouse ischemic model and provided protection from the ischemic injury.²⁴ From a clinical perspective, there are advantages to targeting the single, low-abundance LP enzyme rather than one or more of the different LP recognition components (MBL, ficolins or collectin-11). This is important considering that, besides MBL, in man ficolins are critical in triggering LP activation after stroke.⁵ However, the present study clearly shows that LP activation is not the only route of damage downstream from MBL. As such, we envisage that MASP-2 inhibition should be accompanied by complementary targeting of MBL, to counteract its direct actions, which do not require any associated enzymes, thus boosting therapeutic efficacy.

Conclusion

These findings show for the first time a direct relationship between MBL deposition on ischemic endothelial cells and cell injury, also occurring in the absence of other complement components. MBL, mostly known for its ability as an initiator of the LP of complement activation, may actually act independently from the complement cascade and directly contribute to vascular injury, thus standing as an important molecular target for ischemic stroke.

Funding

The author(s) disclosed receipt of the following financial support for the research, authorship, and/or publication of this article: This work was supported by Fondazione Cariplo, Research conducted by young investigators, [project number 2015-1003]; the Rete Cardiologica of IRCCS of the Italian Ministry of Health, Italy; and by the Italian Ministry of Health, agreement number 43/2017, project code: cc-2015-2365332.

Acknowledgements

We thank Matteo Tironi and Andrea Remuzzi of Biomedical Engineering Department, Istituto di Ricerche Farmacologiche Mario Negri IRCCS, Bergamo, for kindly providing HepG2 cells. We thank Nicolò Panini of Cancer Pharmacology Laboratory, Istituto di Ricerche Farmacologiche Mario Negri IRCCS, Milano, for the technical assistance during the work.


Declaration of conflicting interests

The author(s) declared no potential conflicts of interest with respect to the research, authorship, and/or publication of this article.

Authors' contributions

LN, SF, FO, CP conducted the experiments, analyzed data and wrote the manuscript; AZ analyzed the data; MGDS designed the study, analysed the data, wrote the manuscript.

ORCID iD

Maria-Grazia De Simoni  <https://orcid.org/0000-0002-0259-0003>

Supplemental material

Supplemental material for this paper can be found at the journal website: <http://journals.sagepub.com/home/jcb>

References

1. Gesuete R, Storini C, Fantin A, et al. Recombinant C1 inhibitor in brain ischemic injury. *Ann Neurol* 2009; 66: 332–342.
2. Orsini F, Villa P, Parrella S, et al. Targeting mannose-binding lectin confers long-lasting protection with a surprisingly wide therapeutic window in cerebral ischemia. *Circulation* 2012; 126: 1484–1494.
3. Cervera A, Planas AM, Justicia C, et al. Genetically-defined deficiency of mannose-binding lectin is associated with protection after experimental stroke in mice and outcome in human stroke. *PLoS One* 2010; 5: e8433.
4. Osthoff M, Katan M, Fluri F, et al. Mannose-binding lectin deficiency is associated with smaller infarction size and favorable outcome in ischemic stroke patients. *PLoS One* 2011; 6: e21338.
5. Fumagalli S and De Simoni M-G. Lectin complement pathway and its bloody interactions in brain ischemia. *Stroke* 2016; 47: 3067–3073.
6. Rosa X de la, Cervera A, Kristoffersen AK, et al. Mannose-binding lectin promotes local microvascular thrombosis after transient brain ischemia in mice. *Stroke*. www.ahajournals.org/doi/abs/10.1161/STROKE.AHA.113.004111?url_ver=Z39.88-2003&rfr_id=ori:rid:crossref.org&rfr_dat=cr_pub%3dpubmed (2014, accessed 30 October 2018).
7. Orsini F, Fumagalli S, Császár E, et al. Mannose-binding lectin drives platelet inflammatory phenotype and vascular damage after cerebral ischemia in mice via IL (Interleukin)-1 α . *Arterioscler Thromb Vasc Biol* 2018; 38: 2678–2690.
8. Thornton P, McColl BW, Greenhalgh A, et al. Platelet interleukin-1 α drives cerebrovascular inflammation. *Blood* 2010; 115: 3632–3639.
9. Neglia L, Oggioni M, Mercurio D, et al. Specific contribution of mannose-binding lectin murine isoforms to brain ischemia/reperfusion injury. *Cell Mol Immunol*. Epub ahead of print 9 April 2019. DOI: 10.1038/s41423-019-0225-1.
10. Roos A, Bouwman LH, Munoz J, et al. Functional characterization of the lectin pathway of complement in human serum. *Mol Immunol* 2003; 39: 655–668.
11. Perego C, Fumagalli S and De Simoni M-G. Temporal pattern of expression and colocalization of microglia/macrophage phenotype markers following brain ischemic injury in mice. *J Neuroinflammation* 2011; 8: 174.
12. Ball G, Demmerle J, Kaufmann R, et al. SIMcheck: a toolbox for successful super-resolution structured illumination microscopy. *Sci Rep* 2015; 5: 15915.

13. Zanier ER, Fumagalli S, Perego C, et al. Shape descriptors of the “never resting” microglia in three different acute brain injury models in mice. *Intensive Care Med* 2015; 3: 7.
14. Collard CD, Väkevä A, Morrissey MA, et al. Complement activation after oxidative stress. *Am J Pathol* 2000; 156: 1549–1556.
15. Collard CD, Montalto MC, Reenstra WR, et al. Endothelial oxidative stress activates the lectin complement pathway: role of cytokeratin 1. *Am J Pathol* 2001; 159: 1045–1054.
16. Longhi L, Orsini F, De Blasio D, et al. Mannose-binding lectin is expressed after clinical and experimental traumatic brain injury and its deletion is protective*. *Crit Care Med* 2014; 42: 1910–1918.
17. De Blasio D, Fumagalli S, Orsini F, et al. Human brain trauma severity is associated with lectin complement pathway activation. *J Cereb Blood Flow Metab* 2019; 39: 794–807.
18. Ando Y, Okada H, Takemura G, et al. Brain-specific ultrastructure of capillary endothelial glycocalyx and its possible contribution for blood brain barrier. *Sci Rep* 2018; 8: 17523.
19. van der Pol P, Schlagwein N, van Gijlswijk DJ, et al. Mannan-binding lectin mediates renal ischemia/reperfusion injury independent of complement activation: MBL is cytotoxic to tubular epithelial cells. *Am J Transplant* 2012; 12: 877–887.
20. Garred P, Larsen F, Madsen HO, et al. Mannose-binding lectin deficiency – revisited. *Mol Immunol* 2003; 40: 73–84.
21. Tornabene E and Brodin B. Stroke and drug delivery – in vitro models of the ischemic blood-brain barrier. *J Pharm Sci* 2016; 105: 398–405.
22. Ip WKE, Takahashi K, Ezekowitz RA, et al. Mannose-binding lectin and innate immunity. *Immunol Rev* 2009; 230: 9–21.
23. Montalto MC, Collard CD, Buras JA, et al. A keratin peptide inhibits mannose-binding lectin. *J Immunol* 2001; 166: 4148–4153.
24. Orsini F, Chrysanthou E, Dudler T, et al. Mannan binding lectin-associated serine protease-2 (MASP-2) critically contributes to post-ischemic brain injury independent of MASP-1. *J Neuroinflammation* 2016; 13: 213.